Charge-state dependence of fast heavy-ion-induced desorption yields described in a thermal model

E. Nieschler, B. Nees, and H. Voit
Physikalisches Institut der Universität Erlangen-Nürnberg, D-8520 Erlangen, West Germany
(Received 10 November 1987)

Yields for secondary ions desorbed from valine, tetrabutylammonium tetraphenylborate, and CsI samples by 13- and 30-MeV ^{16}O ions have been measured as a function of the primary-ion charge state. The experimental data can be reproduced in terms of a simple thermal model.

I. INTRODUCTION

Heavy ions with energies of the order of 1 MeV/amu impinging on dielectric samples are able to desorb ions from the sample surface. Interestingly enough, large fragile and otherwise involatile organic molecules can be desorbed in this way. This has been pointed out for the first time by Macfarlane and co-workers.[1] Meanwhile this method has been established as a powerful tool in the mass spectrometry of large biomolecules.[2]

Besides the applied aspect, the question of the underlying desorption mechanism is also of interest. To study this mechanism a number of experiments have been carried out by several groups (see, e.g., Ref. 3) mainly with heavy ions from particle accelerators. Accelerator beams are particularly useful in this respect if the dependence of the desorption yield Y is studied as a function of the primary-ion parameters like energy E, mass m, or incident charge state q_i.

This work deals with the dependence of Y on q_i. This dependence has already been the subject of intensive experimental investigations,[4-8] since it is rather important for the understanding of the desorption mechanism. The experiments[4-8] show that the primary ion interacts with the desorbed molecule not only at the very surface, but also from the interior of the sample, i.e., energy deposited by the primary ion at some distance from the surface is also used up to initiate the desorption of a surface molecule.

This fact prompted us to develop a macroscopic thermal model[9] which explicitly takes into account the interaction from the interior (see also Ref. 10). The model is able to reproduce the dependence of Y on the primary-ion energy as has been shown in Ref. 9 for a number of primary ions impinging on valine and CsI samples. The main purpose of this work is to test the model also with measured $Y(q_i)$ dependences.

II. EXPERIMENTAL TECHNIQUE

$Y(q_i)$ measurements have been performed with the ^{16}O beam of the Erlangen EN tandem accelerator. The beam intensity had to be reduced very drastically (typically 100 primary ions per second) in order not to destroy the sample surface and the surface barrier detector used to stop the primary ions (see the following). A "reduced" beam can easily be obtained at our accelerator since the beam runs through two identical 90° analyzing magnets before entering the target chamber. The second magnet can be used to pick up a charge state q_i different from the charge state q_k selected by the first magnet. The intensity of the beam with charge state q_i can be regulated by varying the pressure between the two magnets.

For the measurements it is essential to ensure that the charge state q_i picked up by the second magnet is not changed before hitting the sample surface. Scattering from residual gas atoms as well as scattering from collimators, slits,[11] and the accelerating grid in the time-of-flight mass spectrometer used to analyze the desorbed secondary ions (see the following) are sources for charge-changing processes. To eliminate these sources we did not use collimators or slits and replaced the accelerating grid by an annular accelerating electrode. Besides this the vacuum between magnet and sample (distance ~ 7 m) was kept below 3×10^{-6} Torr corresponding to $N \leq 1.4\times10^{14}$ cm^{-2} residual gas atoms. This condition ensures that in the worst case (13-MeV ^{16}O ions with $q_i=2$) less than 2% of the primary ions have suffered charge-changing processes (see Fig. 1). The error introduced in this way is of the order of the statistical error of the yield measurements.

The secondary ions were analyzed with a time-of-flight mass spectrometer in which the sample was positioned in such a way that the reduced beam hit the surface from the front side. The angle θ between beam and spectrometer axis is 30 deg. The start signal for the flight-time measurement is obtained from a surface-barrier detector mounted behind the sample. This detector registers the incident primary ions. The stop signal is obtained from a chevron which detects the secondary ions having traversed the flight path (for details see Ref. 13). Secondary ions with masses smaller than the mass of interest were eliminated (by means of the time-of-flight electronic) in order to avoid the "schatten" effect.[14]

The samples investigated are valine, CsI, and tetrabutylammonium tetraphenylborate [in the following the cation with $m=242$ amu and the anion with $m=319$ amu are abbreviated $(TBA)^+$ and $(TPB)^-$, respectively]. They were deposited onto a substrate by means of vacuum evaporation in order to get a good surface structure. The substrate consists of a 40-μg cm^{-2}-thick Formvar foil which was covered by a thin gold layer. Sample

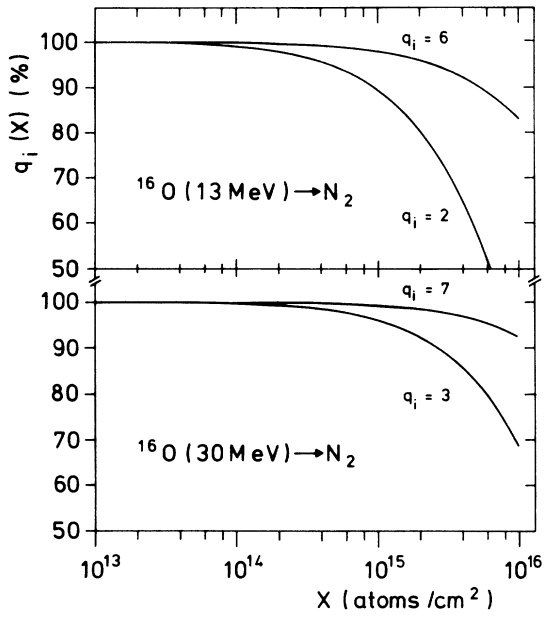

FIG. 1. Variation of the fraction of ^{16}O ions with initial charge state q_i as a function of the thickness X of gaseous nitrogen they have passed through. The curves are calculated from the electron loss and capture data of Ref. 12.

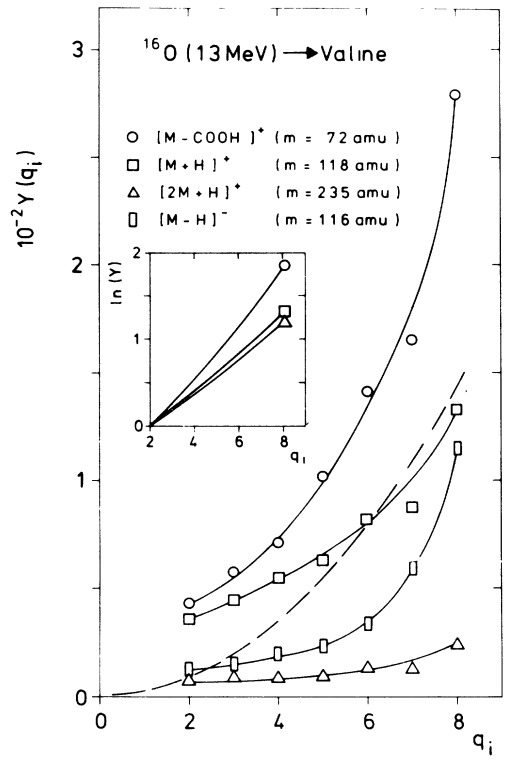

FIG. 2. Yields Y for secondary ions desorbed from a valine sample by 13-MeV ^{16}O primary ions as a function of the initial charge state q_i. Solid lines are guides for the eye. In the inset the lines are normalized to $Y=1$ for $q_i=2$. The dashed line would be obtained for the $[M+H]^+$ yield if the desorption yield were proportional to q_i^2 (note that $q_i=6$ corresponds to the average equilibrium charge $\langle q \rangle$ of a 13-MeV ^{16}O beam). M indicates the valine molecule.

thicknesses were of the order of 15–40 $\mu g\,cm^{-2}$.

Since the accelerator beam had to be tuned again every time a new charge state q_i was selected, it could not be excluded that the experimental conditions changed slightly from data point to data point (a slightly different beam position on the target, a different beam profile). Therefore an additional measurement was performed for each data point using a beam with an equilibrium charge state distribution and a corresponding average charge $\langle q \rangle$. The distribution was generated by means of a thin C foil (≈ 20 $\mu g\,cm^{-2}$) which could be placed in the primary-ion path at a distance of 80 cm from the sample. These measurements were used to normalize the data. The procedure could be cross-checked by measurements with primary ions with an initial charge state q_i equal to the average equilibrium charge $\langle q \rangle$ ($\langle q \rangle \approx 6$ and 7 in the case of 13- and 30-MeV ^{16}O ions, respectively; see Ref. 15). It should be noted that the measured yields are relative yields[16] since the absolute efficiency of the mass spectrometer is not known.

III. EXPERIMENTAL RESULTS AND DISCUSSION

Figures 2–5 show the q_i dependences of the secondary-ion yields for valine, $(TBA)^+$ $(TPB)^-$, and CsI samples obtained for 13- and 30-MeV ^{16}O primary ions. It is obvious from these figures that a pronounced q_i dependence exists: The yields increase with increasing q_i value. This is to be expected since the desorption yield Y depends on the energy deposited by the primary ion which in turn is proportional to the squared ion charge for a fixed energy. Nevertheless, one does not observe a q_i^2 dependence for the yield functions (see the dashed curve in Fig. 2). Among others there are the following reasons for this: (i) the desorption yield is not proportional to the primary-ion energy loss[17–19] and (ii) the energy spent by a surface molecule to leave the surface originates not only from the energy loss deposited at the surface but also from losses deposited in the interior of the sample where charge-changing processes play a role.

The latter aspect has already been used in Refs. 5 and 7 and in an improved way in Ref. 8 to describe measured $Y(q_i)$ dependences. Even though the features of the data are satisfactorily reproduced, one can consider the procedure used in Refs. 5, 7, and 8 only as a zero-order approximation since it neglects the finite desorption probability of a surface molecule and since it takes only approximately into account the effects of the energy dissipation within the sample. It yields, however, a quantity called desorption depth[7] (interaction depth[8]) λ; it determines the maximum depth at which the primary ion still interacts with a surface molecule (via the energy loss) with the result that the molecule is eventually desorbed. It is shown in Refs. 7 and 8 that λ is smaller than the equilibrium depth, i.e., the depth necessary to establish a charge-state equilibrium for the primary-ion beam, and that λ increases with increasing energy loss of the primary ions.

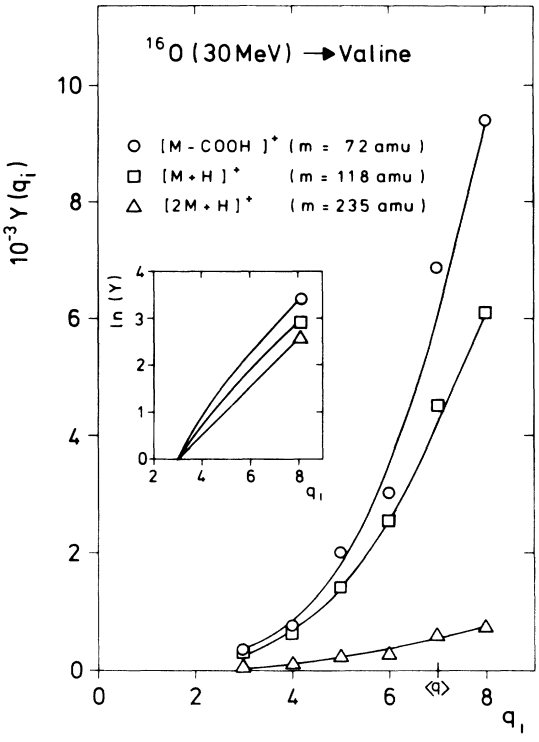

FIG. 3. Yield functions for positive secondary ions desorbed by 30-MeV ^{16}O ions from a valine sample as a function of the initial charge state q_i. The solid lines are guides for the eye. These lines are normalized to $Y=1$ for $q_i=3$ in the inset. For 30-MeV ^{16}O ions $\langle q \rangle$ equals 7.

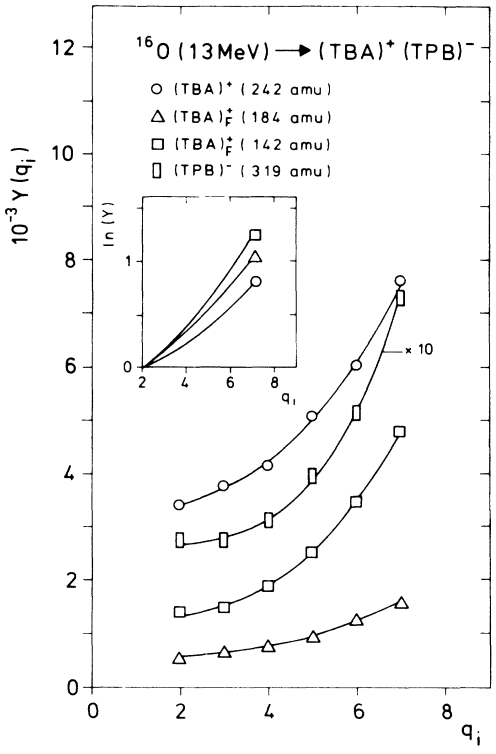

FIG. 4. Yield functions for secondary ions desorbed from a $(TBA)^+$ $(TPB)^-$ sample by 13-MeV ^{16}O ions. $(TBA)_F^+$ ions are fragments of the cation $(TBA)^+$. $(TPB)^-$ is the anion of the sample molecule. The solid lines are guides for the eye. The inset shows the yield functions for positive secondary ions as normalized to $Y=1$ for $q_i=2$.

Besides the quite general dependence of Y on q_i already mentioned, we observe in detail that $Y(q_i)$ differs for different secondary ions desorbed from the same sample. This can be seen in Figs. 2–4, particularly in the insets, which show $\ln[Y(q_i)]$ for different secondary-ion species normalized at the smallest charge state investigated. Obviously $Y(q_i)$ distributions are steeper for negative secondary ions than for positive secondary ions. Besides this the slopes of $Y(q_i)$ distributions for secondary ions with small masses are steeper than those for ions with large masses. The latter observation is in agreement with results of Ref. 8.

A. Macroscopic thermal model

The $Y(q_i)$ dependences measured will be compared in the following with a model which has already been described in detail in Ref. 9, where a discussion of the applicability of the model can also be found. Therefore the concept and the main assumptions of this model are only briefly summarized in the following. For further details the reader is referred to Ref. 9.

It is assumed in the model that molecular ions are desorbed from the very surface of the sample with a prob-

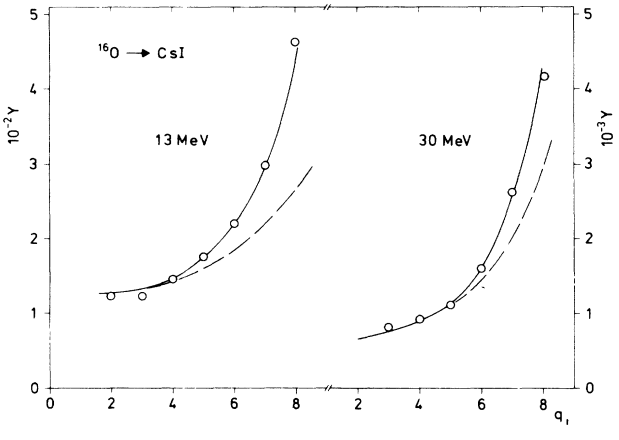

FIG. 5. ^{16}O-induced Cs^+ yields from a CsI sample as a function of the initial charge state q_i. Solid and dashed lines are the predictions of the thermal model. The dashed lines represent calculations performed with a constant value for the surface binding energy ($U_0=6.2$ eV). The solid curves are obtained if U_0 is continuously decreased with increasing q_i values (between 6.2 and 5.0 eV and 6.2 and 5.2 eV in the case of the 13-MeV and 30-MeV data, respectively).

ability proportional to $\exp[-U_0/E_s(r_i^k,t_j)]$, where U_0 is the effective surface binding energy of the molecule and $E_s(r_i^k,t_j)$ is the energy available at the time t_j (the projectile hits the sample at $t_j=0$) at the molecular site having the distance R_i from the primary-ion trajectory and the distance r_i^k from the point P_k (with distance X_k from the surface) lying on the ion path. The source for the energy E_s is the primary-ion energy loss. It is located at P_k. The energy transport from P_k to the molecular site is calculated according to an expression given by Mozumder,[20]

$$E(r,t)=kT_0(1+4\delta t/R_c^2)^{-1}\exp[-r^2/(R_c^2+4\delta t)] , \quad (1)$$

where δ, R_c, and T_0 are the thermal diffusivity, the hot core radius, and the effective temperature of the hot core, respectively. The hot core is defined as a cylindrical region surrounding the heavy-ion track. The hot core radius R_c is given by the range of the low-energy ($E<100$ eV) electrons originating from collisions between heavy-ion and target electrons; R_c depends, according to Ref. 20, on the velocity of the heavy ion and is of the order of 10–40 Å. The temperature T_0 is defined in terms of the linear energy transfer ΔE_l as

$$T_0=\Delta E_l/\pi\rho C_v R_c^2 . \quad (2)$$

The thermal diffusivity δ is given as $\delta=\kappa/\rho C_v$, where κ, ρ, and C_v are the thermal conductivity, the density of the sample, and the specific heat at constant volume, respectively.

With these assumptions one obtains the following expression for the secondary-ion yield Y:

$$Y\propto\sum_{i,j,k} R_i\Delta R\exp[-U_0/E_s(r_i^k,t_j)] , \quad (3)$$

i.e., the yield is proportional to the sum of annular surfaces characterized by the energy E_s and weighted by the desorption probability.

A circular region with radius R_F (the fragmentation radius) on the surface around the ion track is excluded from the sum in Eq. (3) if the desorption yield of fragile molecules is calculated.[21] This region is characterized by a high energy density which causes the molecules in that area to break apart in several small fragment ions. It is obvious that the fragmentation radius R_F depends on the energy deposited by the primary ion. Obviously, for the desorption of Cs^+ ions such an area cannot be excluded. It should be noted that the model takes into account that molecules can be desorbed from layers underneath the sample surface, provided that the molecules in the layers above are already evaporized. The calculations show, however, that this possibility can be neglected for primary ions with relatively small energy loss, in agreement with the experimental results of Ref. 22.

In Ref. 9 it is assumed that the average charge of the incident heavy-ion beam does not change along the ion track in the sample. This assumption does not hold in the present case. As previously mentioned, charge-changing processes take place along the track which have to be involved in the model. This means one has to consider that the energy deposited by the primary ion changes from point to point along the ion trajectory. For this purpose one must know the average charge of the heavy-ion beam at each point P_k along the ion trajectory. It should be noted that the charge-state distribution responsible for this average charge is not an equilibrium distribution since the distances X_k of these points P_k from which considerable amounts of energy still reach the sample surface are small compared to the depth $\langle X\rangle$ necessary to establish a charge-state equilibrium (the maximum distance to be considered for the calculations is of the order of 100–200 Å; see Ref. 9). Nonequilibrium charge-state distributions for low-energy ^{16}O ions in solid matter are measured only in a few cases (see Ref. 23); they are not available for the samples investigated in this work. We have therefore considered the $\{q(X)\}$ distributions for ^{16}O in valine and CsI as a fit parameter in our model calculations.

B. Comparison with valine data

Actual calculations in the framework of the thermal model for arbitrary samples suffer from the fact that the parameters needed are not available in most cases for the organic compounds studied. Fortunately for valine some of the parameters exist in the literature or could be deduced from values of similar compounds. They are listed in Table I together with the parameters for CsI. The same parameters have been used to reproduce the yield functions measured in Ref. 9 where a justification for the applicability of the values can also be found.

Results of the model calculations for yields obtained from a valine sample are shown in Fig. 6. For these calculations a constant hot core radius of $R_c=15$ Å was used. The fragmentation radius R_F was smoothly increased with increasing initial charge state q_i, i.e., with increasing linear energy transfer ΔE_l (see Fig. 7; ΔE_l is proportional to q_i^2). The calculations are performed for an incident angle $\theta=0°$ (calculations performed with the actual angle differ only by a constant factor).

It follows from Fig. 7 that the R_F values for $[M+H]^+$

TABLE I. Parameters used for the model calculations. The values agree with those used in Ref. 9 to describe the dependence of the secondary-ion yield on the primary-ion energy.

Compound	ρ (g/cm^3)	κ (J/cm s K)	C_p (J/g K)	U_0 (eV)	R_c (Å)	R_F (Å)
valine	1.32	2×10^{-4} (30 °C)	1.45 (25 °C)	1.69[$M+H$]$^+$	15	variable
CsI	4.5	1.2×10^{-2} (0°)	0.2 (25 °C)	3.69[$M-H$]$^-$ 6.21	20	0

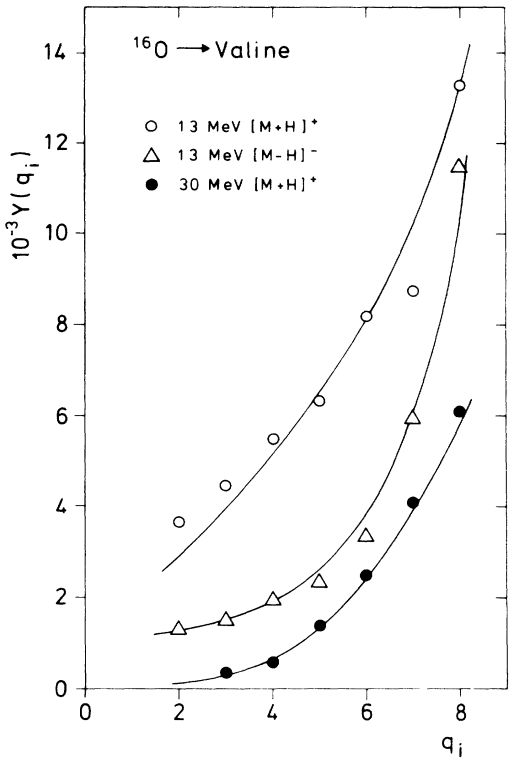

FIG. 6. Results of the model calculations (solid lines) for the ^{16}O-induced desorption from a valine sample. For details see the text.

and $[M-H]^-$ ions are almost identical. Moreover, it turns out that the R_F values for charge states which represent the equilibrium average charge ($q_i = \langle q \rangle$) agree with those values used in Ref. 9 to reproduce the dependence of the yield on the primary-ion energy (these data were obtained for primary ions with an equilibrium charge-state distribution).

Figure 8 shows the energy-loss variation of ^{16}O ions with incident charge q_i as a function of the depth X the ions have penetrated into the valine sample. This functional dependence was used in the model calculations to reproduce the data of Fig. 6. In Fig. 8 actually the ratio $\{q\}^2/v^2$ (it is proportional to the primary-ion energy loss) is shown as a function of the sample thickness X. This X dependence seems to be reasonable, as can be seen by comparing the $\{q(X)\}$ dependences for ^{16}O ions with $q_i = 8$ obtained for 30 MeV in this work and for 40 MeV as obtained in Ref. 23 from a measurement of the nonequilibrium charge-state distribution in a carbon sample. This comparison is made in the inset of Fig. 8. Both $\{q(X)\}$ functions shown exhibit a similar X dependence. The fact that the slope of the 30-MeV function is somewhat steeper than that of the 40-MeV function is to be expected, since the charge-changing processes occur more vigorously for smaller ion energies.[11] The same feature can be observed by comparing the $\{q\}^2/v^2$ functions obtained for 13 and 30 MeV.

There are two additional reasons to believe that the

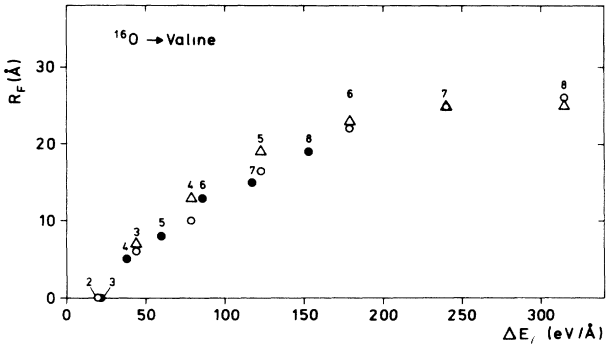

FIG. 7. Dependence of the fragmentation radius R_F used to reproduce the data of Fig. 6 on the linear energy transfer ΔE_l of ^{16}O ions in valine. The initial charge state is indicated by the numbers above the symbol. Circles mark the values for $[M+H]^+$ secondary ions (open circles refer to 13-MeV ^{16}O, full circles to 30-MeV ^{16}O ions). Triangles mark the values for $[M-H]^-$ secondary ions.

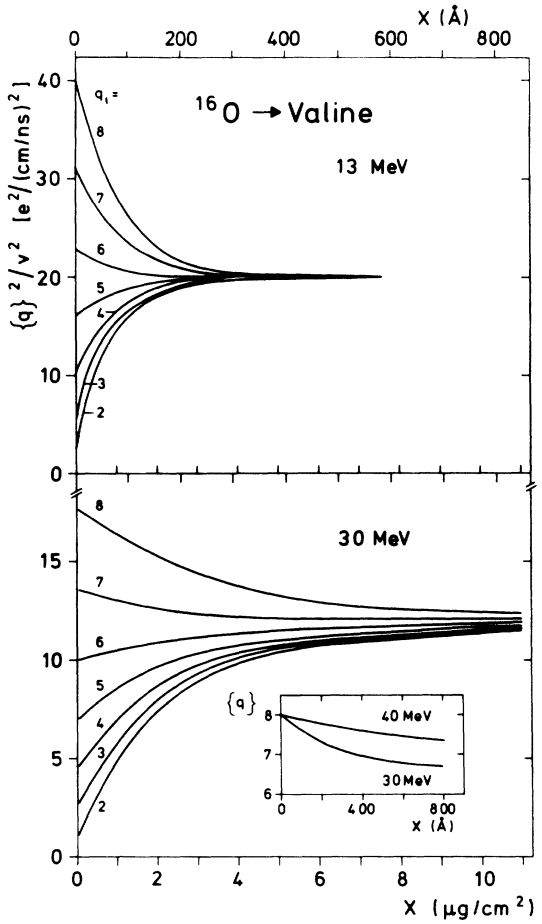

FIG. 8. Dependence of the $\{q\}^2/v^2$ ratio of ^{16}O ions penetrating into a valine sample with different initial charges q_i as a function of the penetration depth X. The curves are obtained from a fit to the experimental data (see the text). $\{q\}$ is the nonequilibrium average charge, v is the ^{16}O velocity. The inset shows $\{q(X)\}$ dependences for $q_i = 8$ as obtained for 30-MeV (this work) and 40-MeV ^{16}O ions (from Ref. 23). In the latter case the curve is deduced from nonequilibrium charge-state measurements performed with a carbon sample.

$\{q(X)\}$ dependences used are reasonable: (i) the nonequilibrium charge $\{q\}$ becomes the equilibrium charge $\langle q \rangle$ for large X values ($\langle q \rangle \approx 6$ and 7 for 13 MeV and 30 MeV, respectively[15]) and (ii) the equilibrium depth $\langle X \rangle$ deducable from the 30-MeV distributions ($\langle X \rangle \geq 10^3$ Å) compares with that obtained for 40-MeV ^{16}O ions in solid carbon.[23]

It should be noted that the slightly different q_i dependences observed for $[M\text{-COOH}]^+$, $[M+\text{H}]^+$, and $[2M+\text{H}]^+$ secondary ions desorbed from the valine sample (see Figs. 2 and 3) can be reproduced with the model calculations if a somewhat smaller fragmentation radius R_F is used for $[M\text{-COOH}]^+$ ions than for $[M+\text{H}]^+$ ions (and a larger radius for $[2M+\text{H}]^+$ ions). This seems reasonable, since one can safely assume that the fragile dimer originates within a surface area which is "colder" than the area from which the $[M\text{-COOH}]^+$ ions are desorbed. The effect of a permanently larger (smaller) R_F value (compared to the standard value) is shown in Fig. 9 which supports the above explanation. The slightly different q_i dependences observed for the sample $(\text{TBA})^+$ $(\text{TPB})^-$ (see Fig. 4) can be explained along the same lines.

C. Comparison with CsI data

The results of model calculations for Cs^+ yields obtained from a CsI sample by bombardment with 13- and 30-MeV ^{16}O ions are given in Fig. 5 (solid and dashed lines). The parameters used for these calculations are given in Table I; they agree with those used in Ref. 9. As in Ref. 9, R_F and R_c were chosen to be 0 Å and 15 Å, respectively. The dependence of the average charge $\{q\}$ of the primary-ion beam on the thickness X of the sample it has passed through was chosen in such a way that at least the yields for small initial charges are reproduced (dashed lines in Fig. 5). The $\{q\}^2$ functions obtained in this way are shown in Fig. 10 (actually the ratio $\{q\}^2/v^2$ is shown). It is obvious from this figure that charge-changing effects occur much more rapidly in CsI compared to valine. This is to be expected, since the electron loss and capture cross sections for ^{16}O projectiles increase with increasing atomic number of the sample.[24]

Obviously the calculations performed as described above (the dashed lines in Fig. 5) underestimate the yields for large incident charge states, i.e., for large energy losses of the primary ions. Similarly, the model calculations of Ref. 9 underestimate the measured Cs^+ yields at small primary-ion energies (i.e., large energy losses) unless the effect of the Coulomb repulsion is taken into ac-

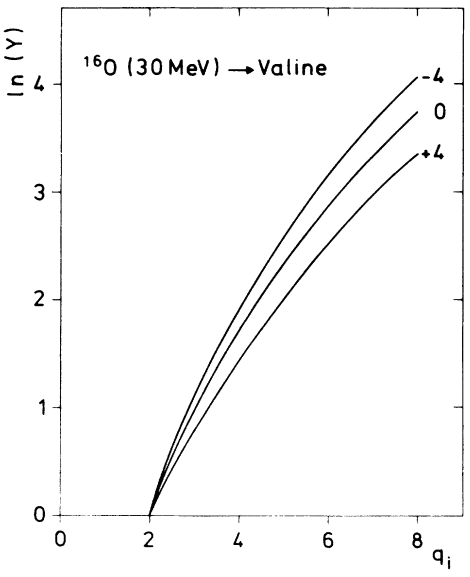

FIG. 9. Model calculations for the ^{16}O (30-MeV) induced desorption for a valine sample. The curve labeled with 0 is identical with the curve labeled with heavy dots in Fig. 6. The curves labeled -4 ($+4$) are calculated with R_F values which are consistently 4 Å smaller (larger) than the R_F values of the curve with label 0.

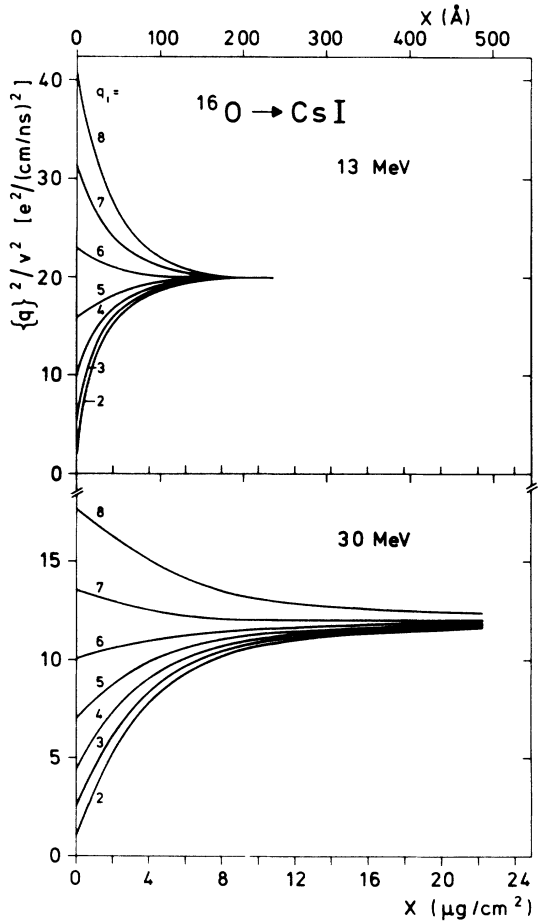

FIG. 10. Dependence of the $\{q\}^2/v^2$ ratio of ^{16}O ions with initial charge q_i penetrating into a CsI sample on the penetration depth X. The curves are obtained from a fit to the experimental data. $\{q\}$ is the nonequilibrium average charge, v is the ^{16}O ion velocity.

count: In the case of large energy losses the primary-ion path is surrounded by a zone with large positive charge density. The positive charges repell the Cs^+ ions. This effect can be involved in the model calculations by decreasing the value of the surface binding energy U_0. If one uses reduced U_0 values (a similar reduction as in Ref. 9) in the case of the large charge states it is possible to reproduce the measured q_i dependence (solid lines in Fig. 5).

IV. CONCLUSION

The dependence of the secondary-ion yield obtained from valine and CsI targets by bombardment with 13- and 30-MeV ^{16}O ions on the primary-ion charge q_i can be described in the framework of a simple thermal model. This model needs only the thermophysical properties and an effective surface binding energy as input parameters. The details of the measured q_i dependence can be accounted for in the model by introducing a fragmentation zone which does not contribute to the yield of fragile molecules and an energy-loss-dependent surface binding energy which allows for the effect of Coulomb repulsion.

ACKNOWLEDGMENT

This work was supported by the Bundesministerium für Forschung und Technologie, Bonn, West Germany.

[1]D. F. Torgerson, R. P. Skowronski, and R. D. Macfarlane, Biochem. Biophys. Res. Commun. **60**, 616 (1974).
[2]B. Sundqvist and R. D. Macfarlane, Mass Spectrom. Rev. **4**, 421 (1985).
[3]Int. J. Mass Spectrom. Ion Phys. **53**, 1 (1983).
[4]P. Håkansson, E. Jayasinghe, A. Johansson, I. Kamensky, and B. Sundqvist, Phys. Rev. Lett. **47**, 1227 (1981).
[5]C. K. Meins, J. E. Griffith, Y. Qin, M. H. Mendenhall, L. E. Seiberling, and T. A. Tombrello, Radiat. Eff. **71**, 13 (1983).
[6]W. Guthier, O. Becker, S. Della-Negra, W. Knippelberg, Y. LeBeyec, U. Weikert, K. Wien, P. Wiesner, and R. Wurster, Int. J. Mass Spectrom. Ion Phys. **53**, 185 (1983).
[7]E. Nieschler, B. Nees, N. Bischof, H. Fröhlich, W. Tiereth, and H. Voit, Radiat. Eff. **83**, 121 (1984).
[8]K. Wien, O. Becker, W. Guthier, S. Della-Negra, Y. LeBeyec, B. Monart, K. G. Standing, G. Maynard, and C. Deutsch, Int. J. Mass Spectrom. Ion Phys. **78**, 273 (1987).
[9]E. Nieschler, B. Nees, H. Voit, P. Beining, and J. Scheer, Phys. Rev. B **37**, 9197 (1988).
[10]R. E. Johnson, B. Sundqvist, P. Håkansson, A. Hedin, M. Salehpour, and G. Säve, Surf. Sci. **179**, 187 (1987).
[11]H. D. Betz, in *Methods of Experimental Physics,* edited by R. Richard (Academic, New York, 1980), Vol. 17.
[12]J. R. Macdonald and F. W. Martin, Phys. Rev. A **4**, 1965 (1971).
[13]E. Nieschler, B. Nees, N. Bischof, H. Fröhlich, W. Tiereth, and H. Voit, Surf. Sci. **145**, 294 (1984).
[14]N. Fürstenau, W. Knippelberg, F. R. Krueger, G. Weiss, and K. Wien, Z. Naturforsch. **32a**, 711 (1977).
[15]R. A. Brown, G. D. Symons, and J. Hall, Nucl. Instrum. Methods **58**, 274 (1968).
[16]P. Dück, W. Treu, H. Fröhlich, W. Galster, and H. Voit, Surf. Sci. **95**, 603 (1980).
[17]B. Nees, E. Nieschler, N. Bischof, H. Fröhlich, K. Riemer, W. Tiereth, and H. Voit, Surf. Sci. **145**, 197 (1984); P. Dück, W. Treu, H. Fröhlich, W. Galster, and H. Voit, *ibid.* **95**, 603 (1980).
[18]P. Håkansson and B. Sundqvist, Radiat. Eff. **61**, 179 (1982).
[19]O. Becker, S. Della-Negra, Y. LeBeyec, and K. Wien, Nucl. Instrum. Methods Phys. Res. **B16**, 3 (1986).
[20]A. Mozumder, Adv. Radiat. Chem. **1**, 1 (1969).
[21]A. Hedin, P. Håkansson, B. Sundqvist, and R. E. Johnson, Phys. Rev. B **31**, 1780 (1985).
[22]G. Säve, P. Håkansson, B. U. R. Sundqvist, R. E. Johnson, E. Söderström, S. E. Lindqvist, and J. Berg, Appl. Phys. Lett. **51**, 1379 (1987).
[23]C. J. Sofield, N. E. B. Cowern, J. Draper, L. Bridwell, J. M. Freeman, C. J. Woods, and M. Spencer-Harper, Nucl. Instrum. Methods **170**, 257 (1980).
[24]U. Scharfer, C. Henrichs, J. D. Fox, P. von Brentano, L. Degener, J. S. Sens, and A. Pape, Nucl. Instrum. Methods **146**, 573 (1977).